

A80-024

Reynolds Number Effects on Aerodynamic Characteristics at Large Angles of Attack

Robert L. Stallings Jr.*

NASA Langley Research Center, Hampton, Va.

20015
20017
40002

An experimental investigation has been conducted to determine the effect of Reynolds number on the aerodynamic characteristics of a body with cruciform wings at large angles of attack. Both pressure distributions and force and moment data have been obtained and are presented for Mach 1.6 and 2.7, Reynolds numbers based on body diameter from approximately 2×10^5 to 28×10^5 , and angles of attack from 0 to 50 deg. In general, the data for the configuration tested show only small effects of Reynolds number throughout the range of test conditions. Also presented and discussed are Schlieren and pressure data that suggest the existence of "wing choking" between the two windward wings for certain roll angles at large angles of attack.

Nomenclature

- A = body cross-sectional area = $\pi D^2/4$
 C_l = rolling moment coefficient = rolling moment/ qAD
 C_N = normal force coefficient = normal force/ qA
 C_n = yawing moment coefficient = yawing moment/ qAD
 C_m = pitching moment coefficient = pitching moment/ qAD
 C_Y = side force coefficient = side force/ qA
 D = body diameter
 M = freestream Mach number
 P = measured surface pressure
 $P_{t,2}$ = total pressure behind a normal shock at freestream Mach number
 q = freestream dynamic pressure
 R_D = freestream Reynolds number based on body diameter
 x = longitudinal distance from nose
 α = angle of attack
 ϕ = model roll orientation ($\phi=0$ corresponds to + fin orientation)

Introduction

THE increased maneuverability requirements of missiles has recently stimulated interest in high angle-of-attack aerodynamics. At these large angles of attack, potential flow methods and linear theories have very limited application, and the missile designer generally resorts to semiempirical methods based on wind-tunnel data for preliminary design purposes. Due to the limited Reynolds number capability of most supersonic wind tunnels and to the small model scale generally required for high angle-of-attack testing, most of the existing high angle-of-attack data at supersonic speeds have been obtained at Reynolds numbers less than flight Reynolds numbers. Since viscosity can have a significant effect on the missile flowfield at these large angles of attack, the effects of Reynolds number on the missile aerodynamic characteristics must be established before these wind-tunnel data can be used with confidence. Therefore, an experimental

investigation was initiated to determine the effect of Reynolds number on the aerodynamic characteristics of a typical cruciform wing-body configuration at large angles of attack.

Models, Instrumentation, and Test Facilities

The cruciform wing-body configuration used in the investigation is illustrated in Fig. 1. Two pressure models and one force model were constructed. The smaller pressure model ($D=0.75$ in.) was instrumented with 101 pressure orifices and was tested at the New York University (NYU) Aerospace and Energetics Laboratory 10.25×8 in. facility.¹ The larger pressure model ($D=1.5$ in.) was instrumented with 225 pressure orifices and was tested at the Langley Unitary Plan wind tunnel (UPWT).² The tests at NYU were conducted at Mach 2.7 and Reynolds numbers based on body diameter from 1.9×10^5 to 23×10^5 . The UPWT pressure tests were conducted at Mach 1.6 and 2.7 and R_D from 1.3×10^5 to 4.0×10^5 . The force model was 1.5 in. in diameter and was instrumented with a six-component strain gage balance for tests in the UPWT and a five-component strain gage balance for tests in the Vought high-speed wind tunnel (HSWT).³ The five-component balance did not have an axial force beam. Moments for both force balance installations were calculated about a point on the model centerline at $x=11.75$ in. The force model was tested at Mach 1.6 and 2.7 for R_D from 1.3×10^5 to 9×10^5 in the UPWT and for R_D from 9×10^5 to 28×10^5 in the Vought HSWT. Shown in Fig. 1b are typical model photographs.

Results and Discussion

Results from the NYU pressure tests have previously been reported¹; therefore, the present paper will concentrate primarily on the force tests and the UPWT pressure tests.

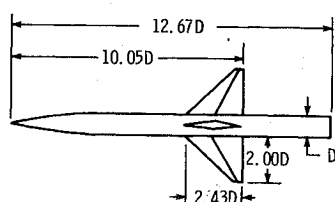
Force Tests

Shown in Fig. 2 are typical measurements of the longitudinal aerodynamic characteristics of the present wing-body model at Mach 1.6 and 2.7 and a roll angle of 22.5 deg. The UPWT data (circular symbols) are presented for $R=2.5 \times 10^5$ and the HSWT data (square symbols) are presented for the maximum test Reynolds number at each Mach number. The model itself is the only factor of commonality between the two sets of data since different balances and stings were used in the two facilities. The data shown in Fig. 2 are representative of the data for the complete range of Reynolds numbers in both facilities and indicate little, if any, effect of Reynolds number on C_N or C_m at either test Mach number. Since similar trends were obtained at $\phi=0$ and 45 deg, these data are not presented. This lack of Reynolds

Presented as Paper 79-0301 at the 17th Aerospace Sciences Meeting, New Orleans, La., Jan. 15-17, 1979; submitted Feb. 20, 1979; revision received July 9, 1979. This paper is declared a work of the U.S. Government and therefore is in the public domain. Reprints of this article may be ordered from AIAA Special Publications, 1290 Avenue of the Americas, New York, N.Y. 10019. Order by Article No. at top of page. Member price \$2.00 each, nonmember, \$3.00 each. Remittance must accompany order.

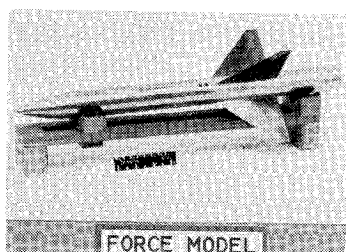
Index categories: Shock Waves and Detonations; Supersonic and Hypersonic Flow; LV/M Aerodynamics.

*Aero-Space Technologist, Supersonic Aerodynamics Branch, High-Speed Aerodynamics Division. Member AIAA.



TYPE-TEST	FACILITY	D, in.	$R_D \times 10^{-5}$	MACH
PRESSURE	NYU	0.75	1.9 TO 23.0	2.70
PRESSURE	UPWT	1.50	1.3 TO 4.0	1.60, 2.70
FORCE	UPWT	1.50	1.3 TO 9.0	
FORCE	HSWT	1.50	9.0 TO 28.0	

a) Configuration and test conditions



b) Photographs of models

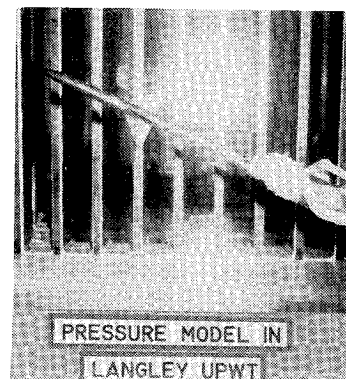
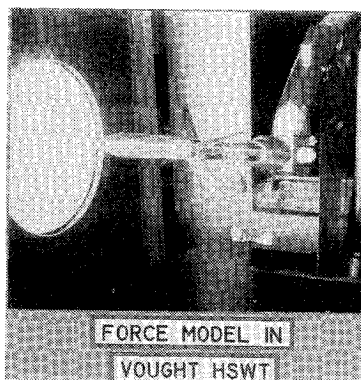


Fig. 1 Description of models and test conditions.

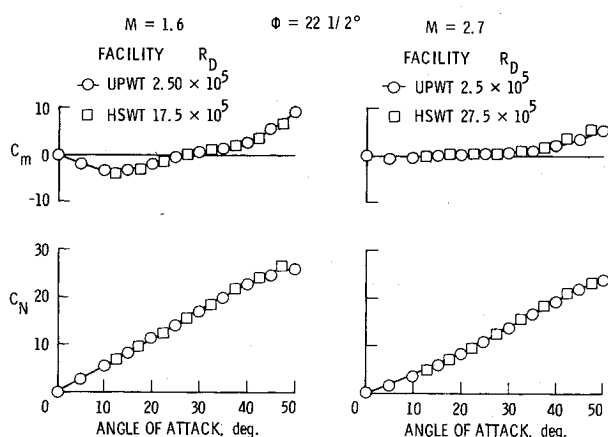


Fig. 2 Effect of Reynolds number on longitudinal aerodynamic characteristics.

number effect is consistent with results from the NYU pressure tests; however, the lack of detailed pressure instrumentation on the small NYU model precluded any firm conclusion on the effect of Reynolds number on its overall aerodynamic characteristics.

The effect of Reynolds number on the lateral characteristics of the model for a roll angle of 22.5 deg is shown in Fig. 3. Results are not presented for $\phi = 0$ and 45 deg since at these conditions all lateral characteristics are essentially zero and invariant with both Reynolds number and angle of attack. The $\phi = 22.5$ deg results shown in Fig. 3 are also relatively independent of Reynolds number but have large nonlinear variations with angle of attack at both test Mach numbers. The onset of the nonlinearity in rolling moment occurs at an angle of attack ($\alpha \approx 15$ deg, $M = 1.6$; $\alpha \approx 35$ deg, $M = 2.7$) corresponding to the onset of an apparent "wing choking" phenomena that occurs between the two windward wings. This phenomenon will be discussed in more detail in the next section.

Pressure Tests

Schlieren and vapor screen studies previously conducted in the UPWT on a cruciform wing-body configuration had shown a very complex flowfield and strong shock wave in-

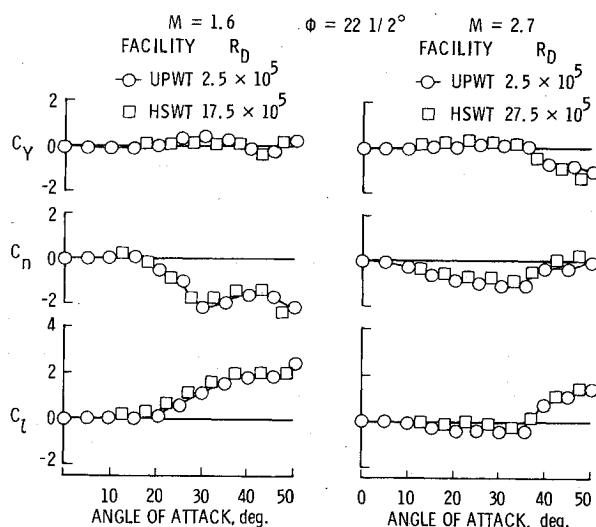


Fig. 3 Effect of Reynolds number on lateral aerodynamic characteristics.

teractions in the wing-body region at large angles of attack. Since local panel loadings in such a wing-body region make large contributions to the overall body forces, an effect of Reynolds number on the local flowfield in this region could result in large effects on the aerodynamics of such a body. Therefore, one objective of the present investigation was to determine the effect of Reynolds number on the local flowfield in the windward wing-body interaction region of a cruciform wing-body configuration at large angles of attack.

Longitudinal pressure distributions in the wing-body interaction region of the present configuration are shown in Fig. 4. The data are presented for Mach 1.6 and 2.7, $\phi = 22.5$ deg, and angles of attack of 20 and 50 deg. The open symbols are data obtained in the UPWT through a Reynolds number range from 1.3×10^5 to 3.8×10^5 and the solid symbols ($M = 2.7$ only) are data obtained at NYU at $R_D = 22.5 \times 10^5$. The data show that large, adverse pressure gradients occur on the body in the vicinity of the wing-root leading edge ($x/D = 7.6$) at the larger angles of attack; however, the pressure distributions are relatively insensitive to Reynolds

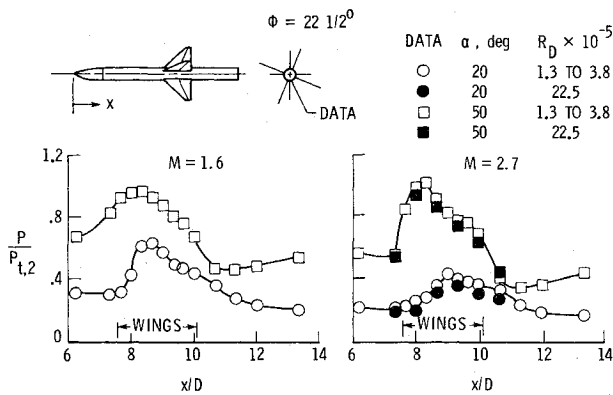


Fig. 4 Pressure measurements on body in wing interaction region.

number through the range of test conditions. Similar results were also obtained at $\phi = 0$ and 45° . This lack of Reynolds number effect may be a result of the large favorable crossflow pressure gradient on the body ahead of the wings venting the large pressures associated with the wing-body interaction region to the lower pressure occurring away from the stagnation line.

Although the primary objective of the present investigation was to determine the effect of Reynolds number on the aerodynamic characteristics and flowfield of a cruciform wing-body configuration, the detailed pressure measurements combined with the force balance measurements have provided a unique set of data that offers an explanation for the anomalous behavior in rolling moment that was shown in Fig. 3 and has also been observed by other investigators (for

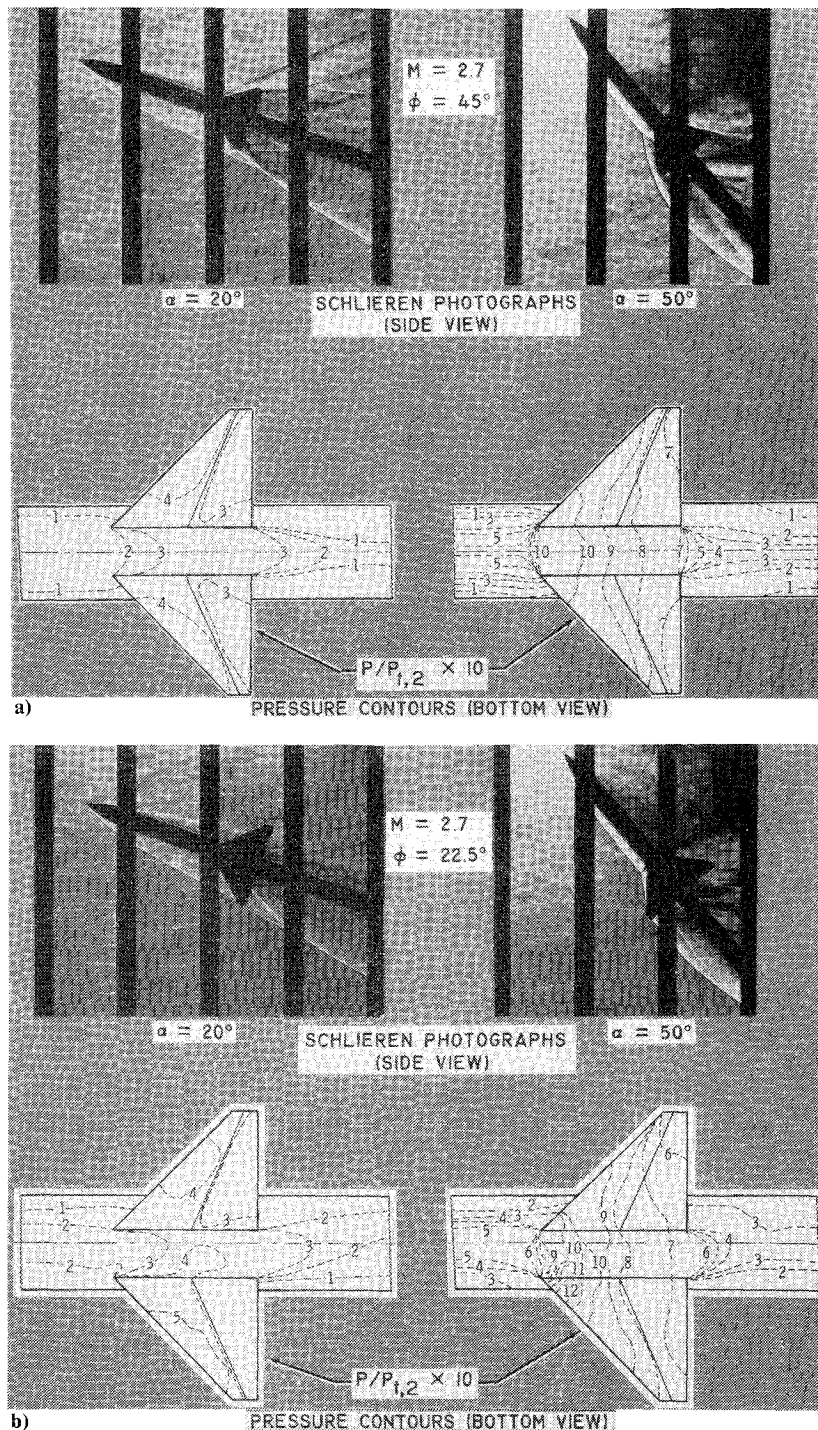


Fig. 5 Effect of wing choking on pressure contours in wing-body interaction region: a) $\phi = 45^\circ$; b) $\phi = 22.5^\circ$.

example, Ref. 4). Presented in Fig. 5 are schlieren photographs and windward pressure contours for the wing-body interaction region of the present configuration at Mach 2.7 and roll angles of 45 and 22.5 deg, Figs. 5a and 5b, respectively. The pressure contours are lines of constant pressure divided by freestream pitot pressure, and they were determined from a pressure orifice matrix consisting of approximately 110 pressure orifices located in the windward wing-body region. The contours are shown for the windward half of the configuration extending through ± 90 deg expansion from the windward stagnation line. The body area shown is the actual surface area rather than a projected area. Also, the windward wings have been rotated about their root chord, such that the true wing planform area is displayed. For $\phi = 45$ deg (Fig. 5a), the pressure contours on the windward wing surfaces at $\alpha = 20$ deg show maximum pressure occurring in the wing leading-edge region with somewhat smaller pressure occurring on the body between the two wings. This type of pressure distribution was generally measured when the wing shock was attached. At $\alpha = 50$ deg, a detached shock occurs ahead of the wings, as shown in the schlieren photograph, and the pressure contours representative of this condition extend from wing to wing across the body, as shown by the pressure measurements. Also at $\alpha = 50$ deg, the maximum measured pressures in the wing-body interaction region are slightly greater than freestream pitot pressure. The similarity of the detached shock, shown in the schlieren photographs for $\alpha = 50$ deg, to the shock formation ahead of a choked inlet has led to this flow phenomenon to be referred to as "fin choking" or "wing choking" (see, for example, Ref. 5). The initial onset of "wing choking" for $M = 2.7$ and $\phi = 45$ deg occurred at $\alpha \approx 35$ deg as determined from both schlieren photographs and pressure measurements.

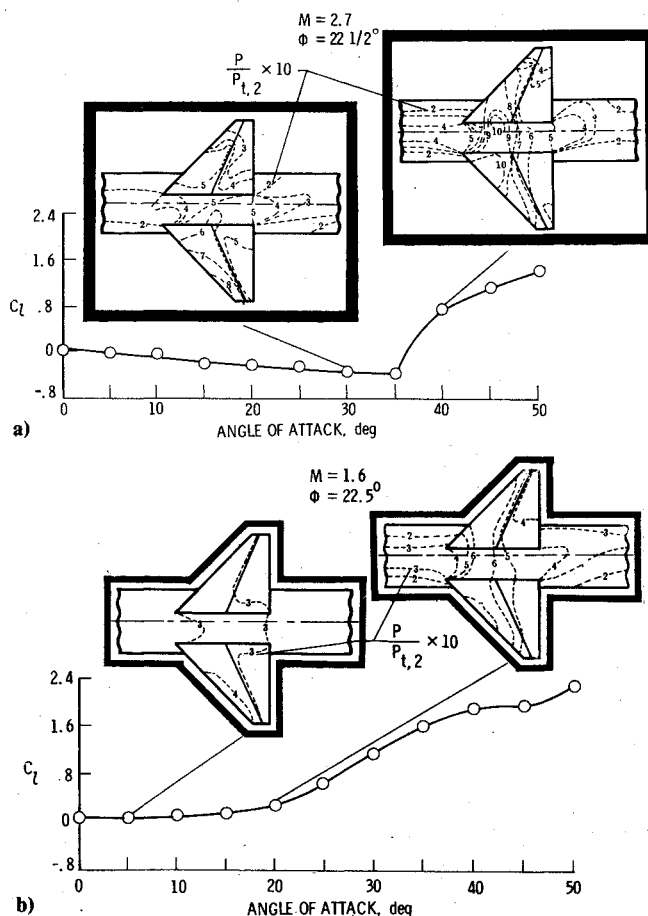


Fig. 6 Effect of wing choking on rolling moment coefficients: a) $M = 2.7$; b) $M = 1.6$.

Data obtained at $\phi = 22.5$ deg are shown in Fig. 5b. At $\alpha = 20$ deg, an attached shock occurs on both windward wings with the greater pressure, as would be expected, occurring on the wing located 67.5 deg from the stagnation line (wing 2), as compared to the wing located 27.5 deg from the stagnation line (wing 3). The effective angle of attack of wing 3 (angle between plane of wing and the freestream velocity vector) is 7.5 deg as compared to 18.4 deg for wing 2. At 50 deg angle of attack, the effective angle of attack for wing 2 is 45 deg and for wing 3 is 17 deg. Therefore, from a flow turning angle criteria, one would expect a detached shock and the resulting larger pressures to occur on wing 2 and an attached shock with corresponding lower pressures on at least part of wing 3. As shown in Fig. 5, the pressure measurements show large pressures representative of a detached shock occurring on both wings 2 and 3 even though wing 3 is at an effective angle of attack much less than required for shock detachment. The presence of a detached shock ahead of wings 2 and 3 is also confirmed by the schlieren photograph. The pressure data indicate that for $\phi = 22.5$ deg and Mach 2.7, this choking phenomena first occurs at $\alpha \approx 35$ deg similar to the $\phi = 45$ deg case. The increase in pressure on the windward side of wing 3 associated with wing choking results in an increase in wing 3 normal force, which results in an increase in rolling moment. This effect is further illustrated in Fig. 6 where the rolling moment coefficient data from Fig. 3 is compared with pressure contour distributions obtained at angles of attack just below and just above the angle of attack that corresponds to the onset of the nonlinear variation in rolling moment. At Mach 2.7 (Fig. 6a), the force data indicate that the nonlinear effects initially occur at $\alpha \approx 35$ deg. Contour plots are, therefore, shown for $\alpha = 30$ and 40 deg. The contours at $\alpha = 30$ deg are representative of attached flow with the larger pressures occurring on wing 2. At $\alpha = 40$ deg, the high pressures on wing 2 extend onto wing 3 indicating wing choking has occurred, resulting in the large increase in rolling moment. At Mach 1.6 (Fig. 6b), the onset of the nonlinear variation in rolling moment occurs at a much smaller angle of attack ($\alpha \approx 15$ deg) and is not as abrupt a variation as was shown at Mach 2.7. The pressure contours shown for $\alpha = 5$ and 20 deg indicate that wing choking has occurred for $\alpha < 20$ deg, which further substantiates the direct effect of wing choking on rolling moment. It is interesting to note that regardless of the wing effective angle of attack, the onset of wing choking occurs at an angle of attack that is approximated by the flow deflection angle corresponding to two-dimensional shock detachment at freestream Mach number. The two-dimensional shock detachment approximation also gives a crude estimate of the onset of the nonlinear rolling moment variation for the Ref. 4 data.

Concluding Remarks

An experimental investigation has been conducted to determine the effect of Reynolds number on the aerodynamic characteristics of a cruciform wing-body configuration at angles of attack up to 50 deg. Both force balance tests and pressure tests were conducted at Mach numbers 1.6 and 2.7, Reynolds numbers based on body diameter from 1.3 to 28×10^5 and roll angles of 0, 22.5, and 45 deg. Results from these tests lead to the following concluding remarks for the cruciform wing-body investigated.

- 1) Force and moment coefficients consisting of normal force, pitching moment, side force, yawing moment, and rolling moment were found to be essentially independent of Reynolds number for the complete range of test conditions.
- 2) No significant Reynolds number effects on pressure coefficient distributions in the windward wing-body interaction region were obtained.
- 3) An anomalous behavior in the variation of rolling moment with angle of attack observed by previous in-

vestigators and also in the present test at a roll angle of 22.5 deg was found to be a result of wing choking between the windward wings.

References

¹Agnone, A.M., Zakkay V., Tory, E., and Stallings, R., "Aerodynamics of Slender Finned Bodies at Large Angles of Attack," AIAA Paper 77-666, 10th Fluid and Plasmadynamic Conference, Albuquerque, N. Mex., June 27-29, 1977.

²Anon., "Manual for Users of the Unitary Plan Wind Tunnel

Facilities of the National Advisory Committee for Aeronautics," NACA, 1956.

³Arnold, J.W., "High Speed Wind Tunnel Facility Handbook," Vought Corporation, Publication No. AER-EIR-13552-C, Revised March 1976.

⁴Monta, W.J., "Supersonic Aerodynamic Characteristics of a Sparrow III Type Missile Model With Wing Controls and Comparison With Existing Tail-Control Results," NASA TP 1078, 1977.

⁵Nielsen, J.N., "Nonlinearities in Missile Aerodynamics," AIAA Paper 78-20, 16th Aerospace Sciences Meeting, Huntsville Ala., Jan. 16-18, 1978